# Enhancement of the Higgs pair production at the CERN LHC: The minimal supersymmetric standard model and extra dimension effects

C. S. Kim
*Department of Physics and IPAP, Yonsei University, Seoul 120-749, Korea*
*and Department of Physics, University of Wisconsin, Madison, Wisconsin 53706*

Kang Young Lee and Jeonghyeon Song
*School of Physics, Korea Institute for Advanced Study, Seoul 130-012, Korea*
(Received 19 September 2000; revised manuscript received 29 January 2001; published 8 June 2001)

Neutral Higgs pair production at the CERN LHC is studied in the MSSM, the large extra dimensional (ADD) model and the Randall-Sundrum (RS) model, where the total cross section can be significantly enhanced compared to that in the SM. The $p_T$, invariant mass and rapidity distributions of each model have been shown to be distinctive: The ADD model raises the $p_T$ and invariant mass distributions at high scales of $p_T$ and invariant mass; in the RS model, resonant peaks appear after the SM contribution dies away; the SM and the MSSM distributions drop rapidly at those high scales; in the ADD and the RS models, the rapidity distributions concentrate more around the center. We conclude that various distributions of Higgs pair production at the LHC with restrictive kinematic cuts would provide one of the most robust signals for the extra dimensional effects.

DOI: 10.1103/PhysRevD.64.015009 PACS number(s): 12.60.Jv, 04.50.+h, 13.85.−t, 13.90.+i

## I. INTRODUCTION

The standard model (SM) has been very successful in explaining experimental signals, including recent results from the CERN $e^+e^-$ collider LEP-II collider [1]. Nevertheless, one of the most important ingredients of the SM, the Higgs mechanism, has not been experimentally probed yet; it is responsible for spontaneous electroweak symmetry breaking, which leads to the mass generation of the $W^{\pm}$ and $Z^0$ gauge bosons and of the SM fermions. Recently, the ALEPH group of the LEP-II has reported the observation of an excess of events by $3\sigma$ in the search for the SM Higgs boson, which corresponds to a Higgs boson mass of about 114 GeV [2]. Since the operation of the LEP-II has been terminated, the decision on whether the observations are only the results of statistical fluctuations or the first signal of Higgs boson production remains suspended until the start of the Fermilab Tevatron II and/or the CERN LHC experiments [3]. Thus it is naturally anticipated that the primary efforts of future collider experiments are to be directed toward the search for the Higgs boson [4].

In particular at hadron colliders, pair production of Higgs bosons plays an important role in the efforts toward understanding the Higgs mechanism [5]. First, it may make possible an experimental reconstruction of the Higgs potential, as the triple self-coupling of Higgs particles is involved. The establishment of the Higgs boson role in electroweak symmetry breaking is crucially dependent on this measurement. Second, the signal-to-background ratio is significantly improved compared to that of single Higgs boson production. The invariant mass scale of *single* Higgs boson production is fixed by the Higgs boson mass, of order $\sim 100\,\mathrm{GeV}$. Thus their detection, through heavy quark decay modes, suffers from large QCD backgrounds. In addition, one viable decay mode $h \to \gamma\gamma$ has a very small branching ratio of order $10^{-3}$ [6]. For *pair* production of Higgs particles, the four $b$ jets in the final states are energetic, reducing the main background $hb\bar{b}$ with soft $b$ jets [7]. Third, this is a rare process in the sense that the effects of physics beyond the SM can remarkably enhance the cross section with respect to that in the SM; the minimal supersymmetric standard model (MSSM) [8] provides some parameter space for the large enhancement of the total cross section, which should accommodate the large Yukawa coupling of $b$ quarks, the resonant decay of $H \to hh$, and/or the dominantly large contribution of the squark loops [7]; extra dimensional models provide tree level diagrams mediated by the Kaluza-Klein (KK) gravitons, leading to large total cross sections. In fact, these new theoretical approaches have drawn extensive attention as candidates for the solution of the gauge hierarchy problem, the existence and stability of the enormous hierarchy between the electroweak and Planck scales. Therefore, it is worth studying the production of a neutral Higgs pair with the effects of the MSSM and the extra dimensional models, and finding the characteristic distribution of each model. We shall restrict ourselves to the procedure at the LHC, which is scheduled to start operating in 2005. In spite of the assurance for the detectibility of the lightest $CP$-even MSSM Higgs boson with $\sqrt{s} \gtrsim 250$ GeV and $\int \mathcal{L} dt \gtrsim 10\ \mathrm{fb}^{-1}$ [9], the LHC has a practical advantage over future $e^+e^-$ linear colliders, since there are no specific plans yet for construction of the latter.

The remainder of the paper is organized as follows. The next section details neutral Higgs pair production at the LHC in the SM, the MSSM, the large extra dimensional [Arkani-Hamed–Dimopoulos–Dvali (ADD)] model [10], and the Randall-Sundrum (RS) model [11]. In Sec. III, we discuss various distributions useful to discriminate effects of each model from the others. The last section represents a brief summary and conclusions.

 

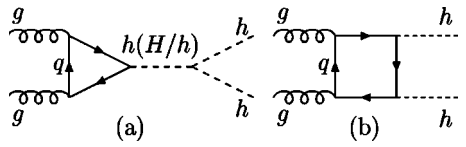


FIG. 1. The Feynman diagrams of the $gg \to hh$ process in the SM (MSSM).

## II. THEORETICAL DISCUSSION AND FORMULAS

The production of a Higgs boson pair at a hadron collider proceeds through several modes: $WW$ fusion, bremsstrahlung of Higgs bosons off heavy quarks, and gluon-gluon fusion. At the LHC, $gg$ fusion is expected to play an important role, since the gluon luminosity increases with beam energy. In this paper, we focus on the process $gg \to hh$, where $h$ is the lightest Higgs boson in each theory.

The invariant amplitude squared is generally written as, in terms of the helicity amplitude $\mathcal{M}_{\lambda_1 \lambda_2}$ for the initial gluon helicities $\lambda_{1(2)}$ [7]:

$$\overline{|\mathcal{M}|^2} = 2 \cdot \frac{1}{4} \cdot \frac{1}{64} \cdot \frac{1}{2} [|\mathcal{M}_{++}|^2 + |\mathcal{M}_{+-}|^2 + |\mathcal{M}_{-+}|^2 + |\mathcal{M}_{--}|^2], \quad (1)$$

where the factor of 2 refers to the color factor $[\mathrm{Tr}(T^a T^b)]^2 = 2$, the factor of 1/4 to the initial gluon helicity average, the factor of 1/64 to the gluon color average, and the final factor of 1/2 to the symmetry factor for the two identically produced Higgs bosons. For the processes with $CP$ conservation, the helicity amplitudes are related as $\mathcal{M}_{++} = \mathcal{M}_{--}$ and $\mathcal{M}_{+-} = \mathcal{M}_{-+}$.

For the numerical analysis, we use the leading order Martin-Roberts-Stirling-Thorne (MRST) parton distribution functions (PDF's) for gluon in a proton [12]. The QCD factorization and renormalization scales $Q$ are set equal to the $hh$ invariant mass, i.e., $\sqrt{\hat{s}}$. The $Q^2$ dependence is expected to be weak in the distribution shapes, which are the main subject of our interest. The center-of-momentum (c.m.) energy at $pp$ collisions is $\sqrt{s} = 14\,\mathrm{TeV}$. And we have employed the kinematic cuts $p_T \geq 25\,\mathrm{GeV}$ and $|\eta| \leq 2.5$ throughout the paper.

### A. In the SM

In the SM, there are two types of Feynman diagrams as depicted in Fig. 1. One is the triangle diagram where a virtual Higgs boson, produced from $gg$ fusion through heavy quark triangles, decays into a pair of Higgs bosons. The other is the box diagram where the Higgs pair is produced through heavy quark boxes. It is to be noted that the triangle diagram incorporates the triple self-coupling of Higgs bosons. For analytic expressions of all the one-loop helicity amplitudes of the process $gg \to hh$, we refer the reader to Refs. [7,5]. Figure 2 shows the total cross section of the SM Higgs pair production at the LHC, as a function of the Higgs boson mass $m_h$. At $m_h \simeq 100\,\mathrm{GeV}$, $\sigma_{\mathrm{tot}}$ is of order 60 fb and decreases rapidly with increasing $m_h$.

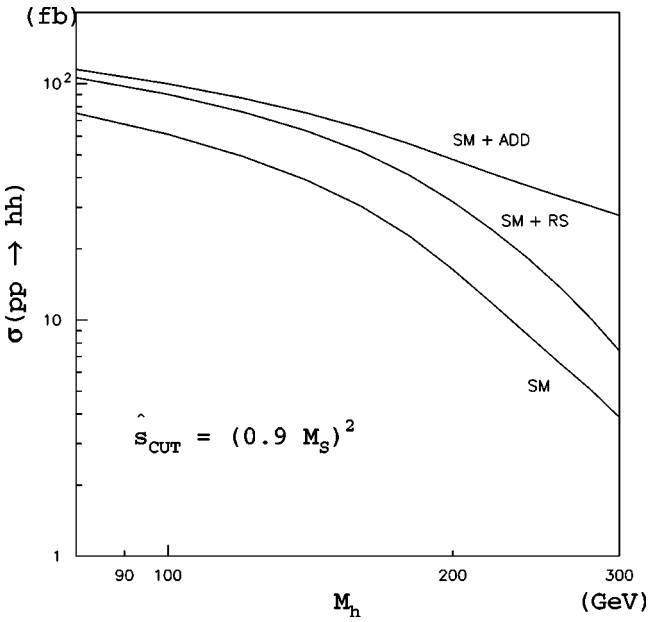


FIG. 2. The total cross section of Higgs pair production as a function of the Higgs boson mass at the LHC with $\sqrt{s} = 14\,\mathrm{TeV}$ in the SM, the ADD and the RS cases. The string scales are set to $M_S = 2.5$ TeV and $\Lambda_\pi = 3$ TeV for the ADD and the RS cases, respectively. The upper bounds $M_{hh} < 0.9 M_S(\Lambda_\pi)$ are employed.

### B. In the MSSM

The existence of a fundamental scalar particle in the SM causes the well-known gauge hierarchy problem. Traditional approaches to the problem are to introduce new symmetries, motivated by the chiral symmetry for light fermion masses and the gauge symmetries for gauge boson masses. Supersymmetry is one of the most popular candidates for this new symmetry.

MSSM Higgs pair production includes distinct contributions coming from the new Higgs and squark sectors, which provide possibilities to greatly enhance the total cross section of the process. First, two doublets and thus two different vacuum expectation values of the Higgs fields allow the Yukawa coupling of the $b$ quark to be compatible with that of the top quark, which corresponds to the large $\tan\beta$ case. The much smaller mass of the $b$ quark may make its loop contribution even larger than the top quark contribution [5]. Second, two Higgs doublets imply the presence of a heavy $CP$-even neutral Higgs boson $H$, which can decay into two light Higgs bosons if kinematically allowed. This resonant contribution $gg \to H \to hh$ is shown to enhance the total cross section with respect to the SM case by about an order of magnitude. Third, the MSSM permits a parameter space where the $\tilde{b}$ or $\tilde{t}$ loop contributions can exceed the SM quark loop contributions by more than two orders of magnitude [7]. For the maximization of squark loop contributions which occurs through the $\tilde{b}$ loops, this parameter space should allow a large value of $\tan\beta$, a considerably light $\tilde{b}_1$ mass, and a large mass of $A$ and/or $|\mu|$. Since the third enhancement possibility has rather restricted parameter space (for example, the squark loop contributions are practically negligible unless $m_{\tilde{b}_1} \lesssim 120$ GeV), we consider only the quark

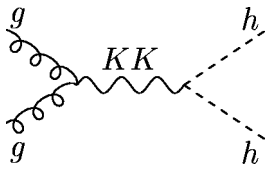


FIG. 3. The Feynman diagrams of the $gg \to hh$ in the ADD and the RS models.

loop contributions, as in Ref. [5]. The corresponding Feynman diagrams are the same as in the SM case, except for the different coupling strengths and the presence of the neutral heavy Higgs boson $H$ (see Fig. 1).

The MSSM total cross section as a function of the Higgs boson mass shows a behavior similar to that of the SM, except for the overall enhancement, as shown in Ref. [5]. As anticipated, the total cross sections in the large and small $\tan\beta$ cases are much increased compared to the SM case. In particular, the large $\tan\beta$ value with $m_h \simeq 100$ GeV leads to an order of magnitude enhancement of the cross section.

### C. In the ADD model

The gauge hierarchy problem has been approached without resort to any new symmetry by Arkani-Hamed, Dimopoulos, and Dvali [10]. One prerequisite of the hierarchy problem itself is removed: The Planck mass is not fundamental; nature allows only one fundamental mass scale $M_S$ which is at the electroweak scale. By introducing the $N \geqslant 2$ extra dimensional compact space, the observed huge Planck mass is attributed to the large volume of the extra space, since $M_{\rm Pl}^2 \simeq M_S^{N+2} R^N$ where the $R$ is the size of the extra dimension. The SM particles cannot escape into the extra space because the matter fields in the model are open strings whose end points are fixed to our four-dimensional world.

Of great interest and significance is that this idea is testable at colliders. The KK reduction from the whole $(4+N)$ dimensions to our four-dimensional world yields towers of massive KK states in the four-dimensional effective theory. Even though the coupling of a KK graviton to ordinary matter fields is extremely suppressed by the Planck scale, a tiny mass splitting $\Delta m_{\rm KK} \sim 1/R$ (which is about $10^{-3}$ eV for the $N=2$ case) induces a summation over all KK states, which compensates for the Planck scale suppression. In addition to the single graviton emission processes as missing energy events [13], the indirect effects of massive graviton exchange on various collider experiments [14] have been extensively studied, as well as possible Lorentz and $CPT$ invariance violations through the change of the metric on the brane [15].

For Higgs pair production through gluon-gluon fusion, there exists a tree level Feynman diagram mediated by spin-2 KK gravitons (see Fig. 3). Based on the effective four-dimensional Lagrangian [16,17], the helicity amplitudes are obtained as

$$\mathcal{M}_{++} = \mathcal{M}_{--} = 0,$$

$$\mathcal{M}_{+-} = \mathcal{M}_{-+} = \frac{16\lambda}{M_S^4}(m_h^4 - \hat{u}\hat{t}), \tag{2}$$

which are to be added to those in the SM. The interference effects between the ADD and the SM are proportional to $1/M_S^4$, which are, at the energy scale below $M_S$, dominant over the pure ADD effects.

There might be a concern about our ignorance of the parton mode $q\bar{q} \to hh$ mediated by KK gravitons. The concern appears reasonable: The characteristic parton energy scale $\sqrt{\hat{s}}$ of the process in extra dimensional models is of the order $M_S \sim$ TeV, unlike a few hundred GeV scale in the SM and the MSSM; the dominant momentum fraction $x$ may not be so small as in the SM and the MSSM cases, and the magnitude of the parton distribution functions of, in particular, the valence quarks becomes substantial. In the following, we have taken into account the parton mode $q\bar{q} \to hh$, which has the square of the scattering amplitude:

$$\overline{|\mathcal{M}|^2}(q\bar{q} \to hh) = \frac{1}{9M_S^8}(\hat{t}-\hat{u})^2(\hat{t}\hat{u} - m_h^4). \tag{3}$$

According to our numerical analysis, the contribution of the $q\bar{q} \to hh$ mode turns out to be at most a few percent of the total cross sections, because the squared amplitude itself is smaller than that of the $gg \to hh$ mode (by a factor of about 1/36) while, at TeV $\sqrt{\hat{s}}$, the PDF of a valence quark and a sea quark is of the same order of magnitude as that of two gluons.

Note that in the parton c.m. frame, the nonzero helicity amplitude can be written as

$$\mathcal{M}_{+-}|_{\text{gg-c.m.}} = -\frac{16\lambda}{M_S^4} p_T^2 \hat{s}, \tag{4}$$

where $p_T$ is the transverse momentum of an outgoing Higgs particle. Unitarity is apparently violated at high energies, which is expected from the use of an effective Lagrangian. It is reasonable that we only consider the region where our perturbative calculations are reliable, which can be achieved by excluding the region with high invariant mass. In Ref. [18], the partial wave amplitudes of the elastic process $\gamma\gamma \to \gamma\gamma$ in the ADD model have been examined, yielding a bound on the ratio $M_S/\sqrt{\hat{s}}$, and a valid region is conservatively found to be $\sqrt{\hat{s}} \leqslant 0.9 M_S$. In the following analyses, we impose an additional kinematic bound such as

$$M_{hh} < 0.9\ M_S.$$

In Fig. 2, we present the total cross section as a function of $m_h$ with $M_S = 2.5$ TeV. As expected from the presence of a tree level diagram in the ADD model, the total cross section is substantially increased with respect to the SM case. For pair production of Higgs bosons with mass 115 GeV, we have obtained

$$\frac{\sigma_{\rm SM+ADD}(m_h = 115\ \text{GeV},\ M_S = 2.5\ \text{TeV})}{\sigma_{\rm SM}(m_h = 115\ \text{GeV})} \approx 1.72. \tag{5}$$

We note that ADD effects lead to a gentle drop-off of the $\sigma_{\rm tot}$ with respect to the Higgs boson mass, contrary to the rapid decrease in the SM. Thus, if the Higgs boson mass is large, the ADD model could still produce a substantially large number of Higgs pairs at the LHC unlike in the SM case.

### D. In the RS model

More recently, Randall and Sundrum have proposed another extra dimensional scenario where, without the *large* volume of the extra dimensions, the hierarchy problem is solved by a geometrical exponential factor, called a warp factor [11]. The spacetime in this model has a single $S^1/Z_2$ orbifold extra dimension with metric

$$ds^2 = e^{-2kr_c|\phi|}\eta_{\mu\nu}dx^\mu dx^\nu + r_c^2 d\phi^2, \tag{6}$$

where $\phi$ is confined to $0 \leqslant |\phi| \leqslant \pi$. The $r_c$ is the compactification radius which is to be stabilized by an appropriate mechanism [19]. Two orbifold fixed points accommodate two three-branes, the hidden brane at $\phi = 0$ and our visible brane at $|\phi| = \pi$ or vice versa. The allocation of our brane at $|\phi| = \pi$ renders a fundamental scale $m_0$ to appear as the four-dimensional physical mass $m = e^{-kr_c\pi}m_0$, which solves the hierarchy problem. And the effective Planck mass is

$$M_{\rm Pl}^2 = (M^3/k)(1 - e^{-2kr_c\pi}),$$

where the $M$ is the five-dimensional Planck scale. Note that all $M_{\rm Pl}$, $k$, and $M$ are of the order of magnitude of the Planck scale.

The compactification of the fifth dimension leads to the following interaction Lagrangian in the four-dimensional effective theory [20]:

$$\mathcal{L} = -\frac{1}{M_{\rm Pl}} T^{\mu\nu}(x) h_{\mu\nu}^{(0)}(x) - \frac{1}{\Lambda_\pi} T^{\mu\nu}(x) \sum_{n=1}^{\infty} h_{\mu\nu}^{(n)}(x), \tag{7}$$

where $\Lambda_\pi \equiv e^{-kr_c\pi} M_{\rm Pl}$. In contrast to the almost continuous KK-graviton spectrum in the ADD model, we have one zero mode of KK gravitons with the coupling suppressed by the Planck scale and the massive KK graviton modes with the electroweak scale coupling $\Lambda_\pi$. The masses of the KK-gravitons are also at the electroweak scale, given by [21]

$$m_n = k x_n e^{-kr_c\pi} = \frac{k}{M_{\rm Pl}} \Lambda_\pi x_n, \tag{8}$$

where the $x_n$'s are the $n$th roots of the Bessel function of order 1.

The scattering amplitudes of the KK-mediated diagrams in the narrow width approximation can be derived from the ADD ones with the following replacement in Eq. (2) [20]:

$$\frac{\lambda}{M_S^4} \to -\frac{1}{8\Lambda_\pi^2} \sum_{n=1}^{\infty} \frac{1}{\hat{s} - m_n^2 + i m_n \Gamma_n}, \tag{9}$$

where the total decay width of the $n$th KK graviton is $\Gamma_n = \rho m_n x_n^2 (k/M_{\rm Pl})^2$, and $\rho$, fixed to be 1, is a model-dependent parameter [20].

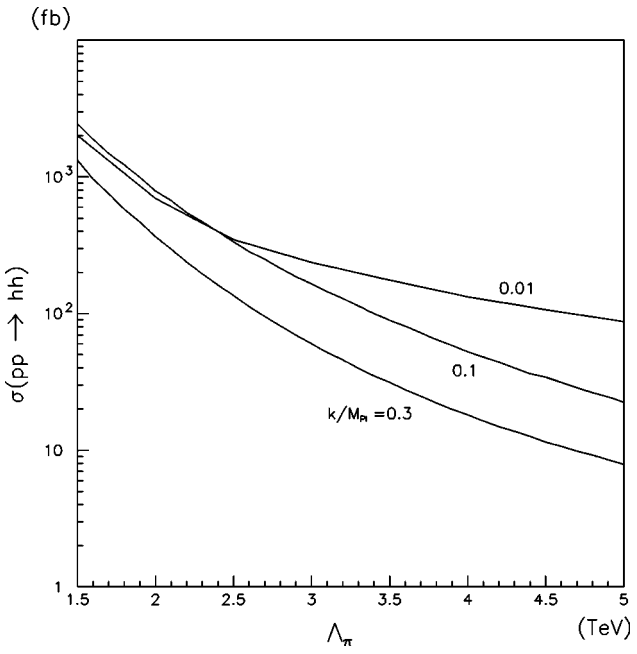


FIG. 4. The total cross sections only with the RS effects as functions of $\Lambda_\pi$, considering three values of the ratio $k/M_{\rm Pl} = 0.01$, 0.1 and 0.3.

The observables based on the four-dimensional effective theory are determined by two parameters $(\Lambda_\pi, k/M_{\rm Pl})$. The value of $k/M_{\rm Pl}$ may be theoretically constrained to be less than about 0.1 [22]: The magnitude of the five-dimensional curvature, $R_5 = -20k^2$, is required to be smaller than $M^2$ $(\simeq M_{\rm Pl}^2)$, so that the classical RS solution derived from the leading order term in the curvature remains reliable. The $\Lambda_\pi$ is expected to be below 10 TeV in order to explain the hierarchy problem. Unlike $M_S$ in the ADD case, $\Lambda_\pi$ does not play the role of a cutoff, relieving the concern about the unitarity violation. According to phenomenological studies of the cross section of $e^+e^- \to \mu^+\mu^-$ in the RS model, only the case with a large value of $k/M_{\rm Pl}$ hints at the unitarity violation; even for $k/M_{\rm Pl} \sim 1$, the unitarity violation can occur at a c.m. energy of several TeV [20]; current LEP-II experiments and the Tevatron run-I have provided a lower bound on $\Lambda_\pi$ of about 1.5 TeV in the case of $k/M_{\rm Pl} = 0.1$.

In Fig. 2, we plot the total cross sections with respect to the Higgs boson mass within the RS model. We set $\Lambda_\pi = 3$ TeV and $k/M_{\rm Pl} = 0.1$. For equity of comparison with the ADD case, we have employed the upper bound $M_{hh} < 0.9\Lambda_\pi$. Though smaller than in the ADD case, the total cross section in the RS case is larger than that in the SM:

$$\frac{\sigma_{\rm SM+RS}(m_h = 115\ \text{GeV},\ M_S = 3\ \text{TeV})}{\sigma_{\rm SM}(m_h = 115\ \text{GeV})} \approx 1.51. \tag{10}$$

The rate of the drop-off of $\sigma_{tot}$ against $m_h$ is similar to the SM case.

In order to demonstrate the dependence of $k/M_{\rm Pl}$ and $\Lambda_\pi$, Fig. 4 shows the total cross section within the RS model as a function of $\Lambda_\pi$, considering three values of the ratio $k/M_{\rm Pl} = 0.01$, 0.1 and 0.3. The Higgs boson mass is set to 100 GeV

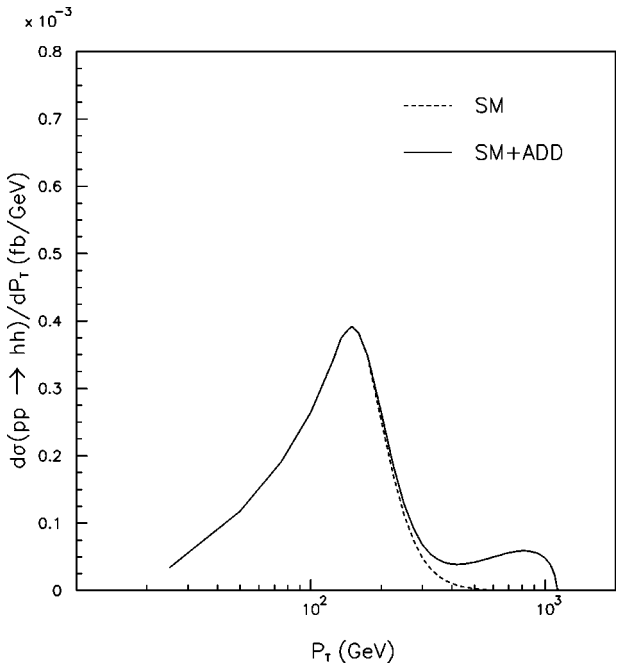


FIG. 5. The $p_T$ distributions of Higgs pair production in the SM and the ADD cases.

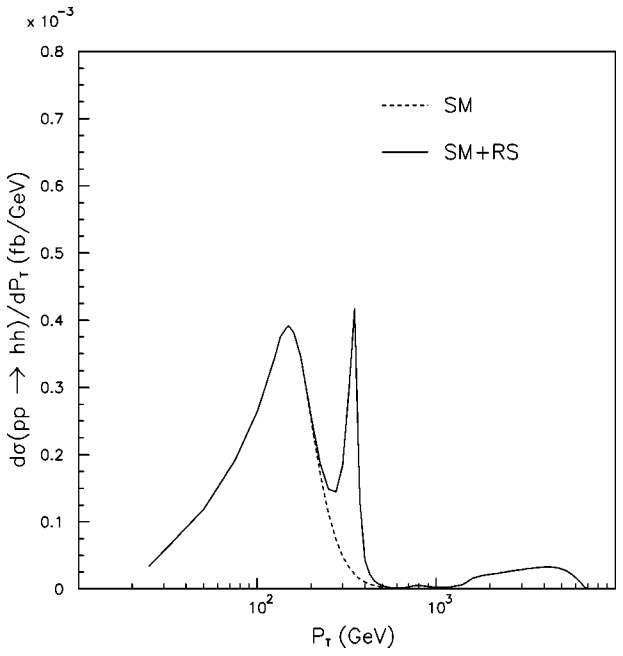


FIG. 6. The $p_T$ distributions of Higgs pair production in the SM and the RS cases.

and the upper bound in $M_{hh}$ is not applied. As $\Lambda_\pi$ increases, $\sigma_{\rm tot}$ drops rapidly. And it can be seen that a smaller value of the ratio $k/M_{\rm Pl}$ produces a larger cross section. This is due to the fact that the amplitude squared in the narrow width approximation is inversely proportional to $(k/M_{\rm Pl})^4$ at each resonance, which yields a dominant contribution.

### III. NUMERICAL DISCUSSION AND DISTRIBUTIONS

In the previous section, we have shown the possibilities of Higgs pair production being greatly enhanced at the LHC. In such circumstances, it is worthwhile to search for appropriate distributions which would enable us to distinguish the contributions of one model from the others. In a numerical analysis of the distributions, we have employed the following parameters: The Higgs boson mass is set equal to 100 GeV; in the MSSM, $\tan\beta=30$, $\mu=-640$ GeV, $M_{\tilde{t}}=M_{\tilde{b}}=1000$ GeV, and $A_t=A_b=-410$ GeV; in the ADD model, $M_S=2.5$ TeV; in the RS model, $\Lambda_\pi=3$ TeV and $k/M_{\rm Pl}=0.1$.

In Fig. 5, we present the $p_T$ distributions in the SM and the ADD cases. While the SM $p_T$ distribution peaks at around 150 GeV and drops rapidly with increasing $p_T$, ADD effects slowly increase the distribution with increasing $p_T$ in the high-$p_T$ region. Note that the absence of a differential cross section at $p_T \gtrsim 1$ TeV is due the employment of the upper bound on $M_{hh}$. Figure 6 shows the $p_T$ distributions in the SM and the RS cases. The presence of Kaluza-Klein gravitons in the RS model leads to a clear shape of the resonance. We caution the reader that the $p_T$ axis is plotted on a logarithmic scale: Even if $d\sigma^{\rm SM+\,RS}/dp_T$ at $p_T>300$ GeV (which practically vanishes in the SM) is smaller than that at $p_T<300$ GeV by an order of magnitude, the extensive contribution in the high-$p_T$ region renders the total cross section substantially enhanced. In Fig. 7, we demonstrate the MSSM $p_T$ distribution for the large $\tan\beta$ case. It drops rapidly with increasing $p_T$, as in the SM case, while it peaks at around 25 GeV, lower than in the SM case. The magnitude of the differential cross section is about 20 times larger than that in the SM case.

Figure 8 illustrates the invariant mass distributions of the Higgs pair in the SM and the ADD cases. The SM case, where the top quark loop contributions are dominant, peaks at around the threshold $\sqrt{\hat{s}}\simeq 2m_t$. The ADD effects gently

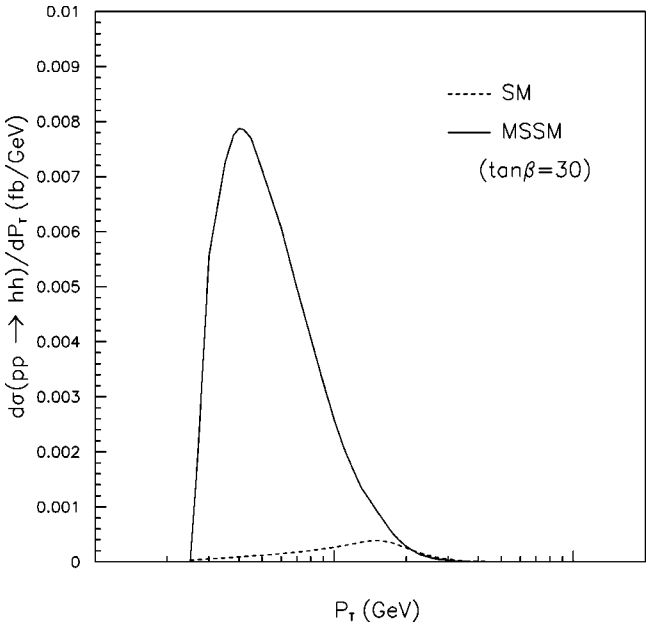


FIG. 7. The $p_T$ distributions of Higgs pair production in the SM and the MSSM.

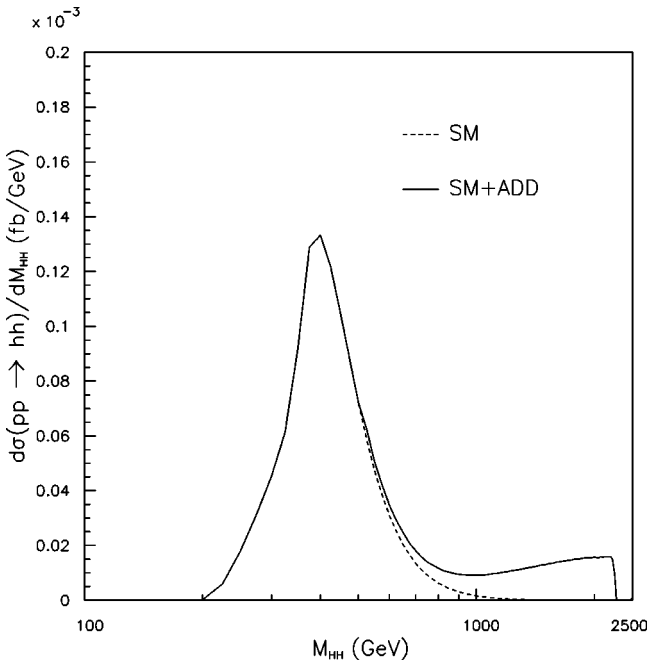


FIG. 8. The $M_{hh}$ distributions of Higgs pair production in the SM and the ADD cases.

increase the $M_{hh}$ distribution in the high-$M_{hh}$ region. It is expected that the blind application of the effective Lagrangian in Eq. (4) without any upper bound on $M_{hh}$ would yield a continual increase in the $M_{hh}$ distributions, which would lead to an apparent violation of unitarity. We display the $M_{hh}$ distribution of the RS case in Fig. 9. The high resonance peak in addition to the SM distribution implies the first KK state of gravitons with $m_1 \simeq 750$ GeV. While in the $e^+e^- \rightarrow \mu^+\mu^-$ process the KK gravitons appear as almost regularly spaced peaks [20], the hadronic convolution of the parton level processes obscures successive and separated peaks such as the classical KK signature. Figure 10 displays the $M_{hh}$ distribution of the MSSM case with large $\tan\beta$, which possesses the dominant contributions from $b$ quarks. Thus a peak appears just above the kinematic threshold, $\sqrt{\hat{s}} \simeq 2m_h$.

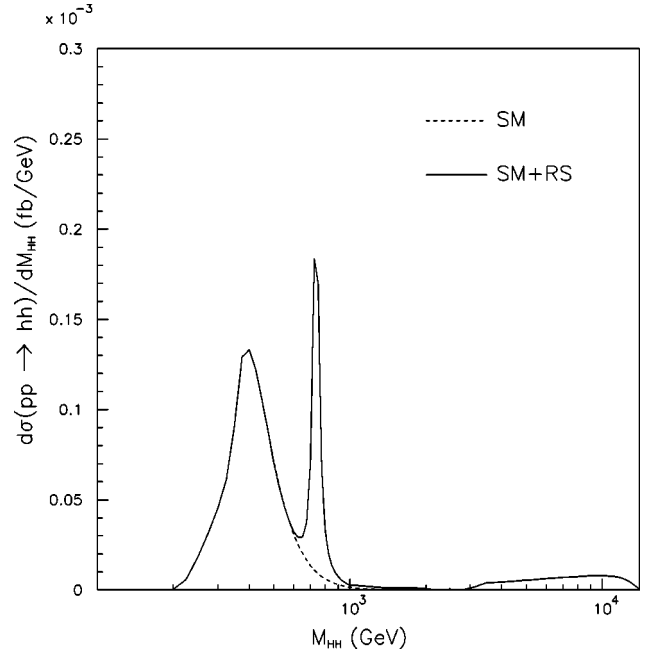


FIG. 9. The $M_{hh}$ distributions of Higgs pair production in the SM and the RS cases.

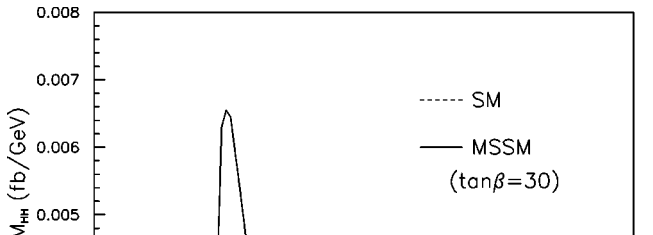


FIG. 10. The $M_{hh}$ distributions of Higgs pair production in the SM and the MSSM.

Finally, we illustrate the rapidity distributions in Fig. 11. It can be seen that the extra dimensional models produce a Higgs pair somewhat more centrally in the rapidity than the SM and the MSSM do. A more restrictive cut on $\eta$, such as

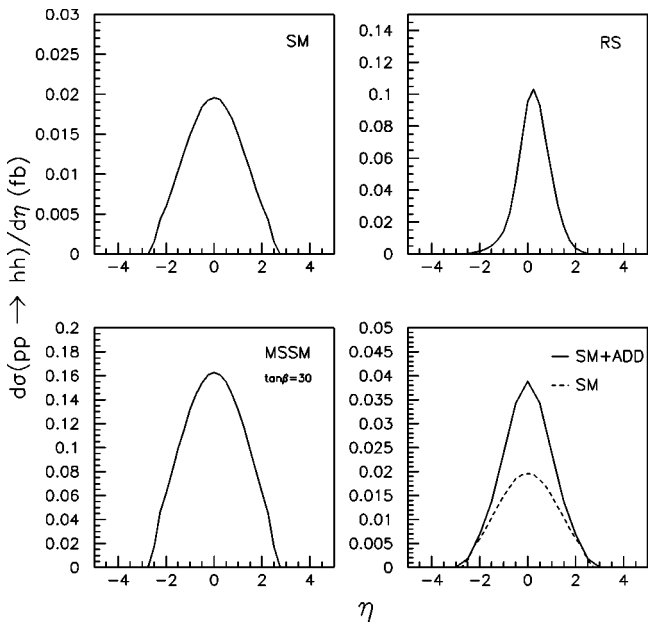


FIG. 11. The $\eta$ distributions in the SM, the MSSM, the RS and the ADD cases.

$\eta \leqslant 1.0$, would eliminate a substantial portion of the SM and the MSSM contributions.

## IV. CONCLUSIONS

The pair production of neutral Higgs bosons from gluon-gluon fusion at the LHC has been studied in the SM, the MSSM, the large extra dimensional model and the Randall-Sundrum model. We have shown that both the supersymmetric and extra-dimensional models can substantially enhance the total cross section of Higgs pair production. In the MSSM case, the large $\tan\beta$ value makes it possible that the *b*-quark contribution dominates over the top quark contribution and over the resonant decay of a heavy Higgs particle into two light Higgs particles. The extra dimensional models allow contributions from tree level Feynman diagrams mediated by Kaluza-Klein gravitons, which significantly increase the total cross section. Since the ADD model has been shown to violate partial wave unitarity at high energies, we have employed an upper bound on the invariant mass of two Higgs bosons, which is obtained from an analysis of the *J* partial wave amplitudes of the elastic process $\gamma\gamma \rightarrow \gamma\gamma$. In addition, we have shown that the total cross section in the ADD case with an upper bound on $M_{hh}$ decreases gently with increasing Higgs boson mass, whereas those in the SM, the MSSM and the RS cases decrease rapidly.

If Higgs pairs are produced at hadron colliders at a much higher rate than in the SM, the three non-standard models considered here are good candidates for an explanation. We have shown the $p_T$, invariant mass and rapidity distributions of each case. The distribution shapes are shown to be different for each model, providing valuable criteria to distinguish one model from the others. The $p_T$ distribution in the SM peaks and drops rapidly; in the MSSM, and in the large $\tan\beta$ case, it peaks just above the threshold of $p_T$ and also drops rapidly; the ADD effects induce a slow increase after the SM peak; the RS effects can be discovered by the presence of a resonance peak. The invariant mass distributions are similar to the $p_T$ distributions: The SM and the MSSM distributions have peaks at around a few hundred GeV; the ADD effects gently increase the $M_{hh}$ distribution at high energies; the RS contribution yields a series of resonant peaks. Therefore, restrictive cuts on $p_T$ and $M_{hh}$ would eliminate the main contributions of the SM and the MSSM cases, which provides one of the most straightforward methods to detect the existence of low scale quantum gravity effects. Finally, the rapidity distributions in the ADD and the RS models show significantly narrow peaks around $\eta = 0$, which implies large contributions in the high-$p_T$ region.

## ACKNOWLEDGMENTS

We thank G. Cvetic and P. Zerwas for a careful reading of the manuscript and valuable comments. The work of C.S.K. was supported in part by the Seo-Am (SBS) Foundation, in part by BK21 Program, SRC Program and Grant No. 2000-1-11100-003-1 of the KOSEF, and in part by KRF grants, Project No. 2000-015-DP0077. The research of J.S. was supported by the BK21 Program for the Seoul National University.

[1] For a recent review, see, e.g., J. Ellis, hep-ph/0007161.
[2] ALEPH Collaboration, R. Barate *et al.*, Phys. Lett. B **295**, 1 (2000).
[3] J. Ellis, hep-ex/0011086.
[4] See, e.g., J. F. Gunion, H. E. Haber, G. L. Kane, and S. Dawson, *The Higgs Hunter's Guide* (Addison-Wesley, Reading, MA, 1990).
[5] T. Plehn, M. Spira, and P. M. Zerwas, Nucl. Phys. **B479**, 46 (1996); **B531**, 655(E) (1998).
[6] J. F. Gunion, G. Gamberini, and S. F. Novaes, Phys. Rev. D **38**, 3481 (1988).
[7] A. Belyaev, M. Drees, O. J. P. Éboli, J. K. Mizukoshi, and S. F. Novaes, Phys. Rev. D **60**, 075008 (1999).
[8] For a review, see H. E. Haber and G. L. Kane, Phys. Rep. **117**, 75 (1985).
[9] V. Barger, K. Cheung, R. J. N. Phillips, and A. L. Stange, Phys. Rev. D **47**, 3041 (1993); A. Djouadi, W. Kilian, M. Mühlleitner, and P. M. Zerwas, Eur. Phys. J. C **10**, 27 (1999); D. J. Miller and S. Moretti, hep-ph/0001194.
[10] N. Arkani-Hamed, S. Dimopoulos, and G. Dvali, Phys. Lett. B **429**, 263 (1998); Phys. Rev. D **59**, 086004 (1999); I. Antoniadis, N. Arkani-Hamed, S. Dimopoulos, and G. Dvali, Phys. Lett. B **436**, 257 (1998).
[11] L. Randall and R. Sundrum, Phys. Rev. Lett. **83**, 3370 (1999); **83**, 4690 (1999).
[12] A. D. Martin, R. G. Roberts, W. J. Stirling, and R. S. Thorne, Eur. Phys. J. C **14**, 133 (2000).
[13] E. A. Mirabelli, M. Perelstein, and M. E. Peskin, Phys. Rev. Lett. **82**, 2236 (1999).
[14] J. L. Hewett, Phys. Rev. Lett. **82**, 4765 (1999); C. Balazs, H.-J. He, W. W. Repko, and C.-P. Yuan, *ibid.* **83**, 2112 (1999); K. Cheung and W.-Y. Keung, Phys. Rev. D **60**, 112003 (1999); K. Agashe and N. G. Deshpande, Phys. Lett. B **456**, 60 (1999); T. G. Rizzo and J. D. Wells, Phys. Rev. D **61**, 016007 (2000); T. G. Rizzo, *ibid.* **60**, 075001 (1999); K. Y. Lee, H. S. Song, and J. Song, Phys. Lett. B **464**, 82 (1999); K. Y. Lee, H. S. Song, J. Song, and C. Yu, Phys. Rev. D **60**, 093002 (1999); K. Y. Lee, S. C. Park, H. S. Song, J. Song, and C. Yu, *ibid.* **61**, 074005 (2000).
[15] G. Dvali and M. Shifman, Phys. Rep. **320**, 107 (1999); G. Cvetic, S. K. Kang, C. S. Kim, and K. Lee, Phys. Rev. D **62**, 057901 (2000).
[16] T. Han, J. D. Lykken and R. Zhang, Phys. Rev. D **59**, 105006 (1999).
[17] G. F. Giudice, R. Rattazzi, and J. D. Wells, Nucl. Phys. **B544**, 3 (1999).
[18] O. J. Eboli, T. Han, M. B. Magro, and P. G. Mercadante, Phys. Rev. D **61**, 094007 (2000).

[19] W. D. Goldberger and M. B. Wise, Phys. Rev. Lett. **83**, 4922 (1999).
[20] H. Davoudiasl, J. L. Hewett, and T. G. Rizzo, Phys. Rev. Lett. **84**, 2080 (2000).
[21] W. D. Goldberger and M. B. Wise, Phys. Rev. D **60**, 107505 (1999).
[22] H. Davoudiasl, J. L. Hewett, and T. G. Rizzo, Phys. Lett. B **473**, 43 (2000); H. Davoudiasl, J. L. Hewett, and T. G. Rizzo, Phys. Rev. D **63**, 075004 (2001).